Eco-friendly methanesulfonic acid and sodium salt of dodecylbenzene sulfonic acid doped cross-linked chitosan based green polymer electrolyte membranes for fuel cell applications

V. Vijayalekshmi, Dipak Khastgir

www.elsevier.com/locate/memsci

PII: S0376-7388(16)31278-9
DOI: http://dx.doi.org/10.1016/j.memsci.2016.09.058
Reference: MEMSCI14779

To appear in: *Journal of Membrane Science*

Received date: 11 August 2016
Revised date: 27 September 2016
Accepted date: 28 September 2016

Cite this article as: V. Vijayalekshmi and Dipak Khastgir, Eco-friendly methanesulfonic acid and sodium salt of dodecylbenzene sulfonic acid doped cross-linked chitosan based green polymer electrolyte membranes for fuel cell applications, *Journal of Membrane Science* http://dx.doi.org/10.1016/j.memsci.2016.09.058

Eco-friendly methanesulfonic acid and sodium salt of dodecylbenzene sulfonic acid doped cross-linked chitosan based green polymer electrolyte membranes for fuel cell applications

V. Vijayalekshmi, DipakKhastgir*

Rubber Technology Centre, Indian Institute of Technology Kharagpur, West Bengal, 721302, India

***Corresponding Author:** Tel.:+91-3222-282292;khasdi@rtc.iitkgp.ernet.in

Abstract

Methanesulfonic acid (MSA) and sodium salts of dodecylbenzene sulfonic acid (SDBS) were introduced into chitosan matrix to improve the proton conductivity and solvent stability through cross-linking with sulfuric acid. 15 wt % MSA doped chitosan membrane shows a proton conductivity of 2.86×10^{-4} S/cm at 100°C, but when doped with 10 wt% SDBS, the conductivity of 4.67×10^{-4} S/cm was obtained at the same temperature. The MSA and SDBS doped membranes exhibited better performance compared to pristine chitosan (CS) membrane in terms of mechanical properties and electrical resistance. In addition, the doped membranes are thermally stable up to 260°C. Thus doping of chitosan with MSA and SDBS is found to provide an efficient route to improve thermal stability, mechanical properties and proton conductivity required for polymer electrolyte membranes for fuel cell applications. Moreover, the cost effectiveness and eco – friendliness of CS-MSA and CS-SDBS membranes make their applicability in fuel cell more attractive than the state – of – art (Nafion).

Keywords: Chitosan, fuel cell, polymer electrolyte membrane, proton conductivity

1. Introduction

The proton exchange membrane fuel cells (PEMFCs) have received much attention as a source of clean energy for transportation and portable electronic applications owing to their high energy conversion efficiency and better environmental impact [1-2]. Among the various types of energy devices, the direct methanol fuel cells (DMFCs) are found to be very suitable for portable and transportation applications due their ease of fuel design applicability [3]. The proton exchange

membranes (PEMs), also known as polymer electrolyte membranes are the heart of PEMFCs, and they function as an electrolyte for transferring exclusively proton from anode to cathode and provide barrier to electrons and fuel crossover [4]. An ideal PEM material must have high proton conductivity, good mechanical strength, high fuel crossover resistance, superior thermal and chemical stability and low electric conductivity required for a solid electrolyte for fuel cell [5-7]. Typically, Nafion (a perfluorinated ionomer) based membranes have been considered as the state-of-art as commercial polymer electrolyte membranes in fuel cells by their superior proton conductivity and physicochemical properties. However, high cost, poor fuel barrier properties and instability at operating temperature above 80°C (due to dehydration) have limited their commercial applications. Further, the safe disposability leading to natural biodegradation after useful life is also an important consideration for any useful polymeric materials [8-10].

The cost effective and eco – friendly polymer electrolyte membranes derived from renewable sources can be a promising substitute for common synthetic polymers used in electrochemical devices such as Nafion and sulfonated engineering polymers (sulfonated poly(ether ether ketone), polyvinylidene fluoride, polystyrene, poly(arylene ether sulfone), etc.) [11]. In recent years, chitosan has been widely used as a promising low cost material as proton exchange membranes due to their abundance in the environment with biodegradable, biocompatible and non-toxic nature, low electrical conductivity and methanol permeability. Chitosan is a copolymer consisting of N-acetyl 2-amino glucosamine and D-glucosamine. Furthermore, chitosan based materials exhibit good chemical and thermal stability even up to 200 °C with an acceptable mechanical strength, required for fuel cell operation. However, the pristine chitosan has low conductivity due to the absence of mobile hydrogen ions in its structure. Very low proton conductivity (~10^{-9}S/cm) has been reported in dry chitosan film without any structural modification [12,13]. The presence of functional groups like amine and hydroxyl in the chitosan polymer structure provide scope for further modification to tailor its properties [14-16]. The facile and efficient approach to improve the proton conductivity of chitosan membranes is through doping using acid or inorganic salt [12,13,15,17-20]. These studies show that the proton conductivity of the chitosan membranes could be improved while maintaining its good mechanical, thermal and chemical stability, through cross-linking and appropriate doping.

Methanesulfonic acid (MSA) and sodium salts of dodecylbenzene sulfonic acid (SDBS) are well known as electrochemically active materials having strong acidity and high proton conductivity. SO_3H

groups in these sulfonic acids can provide additional charge hoping sites for proton migration via the Grotthuss mechanism at high temperature. The electrostatic interaction between sulfonic acid groups with the basic amine group of chitosan help in proton transportation with low energy barrier. This further enhances mechanical and thermal stability of the system [21]. In addition, biodegradability and hence the green characteristics of MSA and SDBS reduces the environmental impact [22-24].

PEMs (proton exchange membranes) with high ion exchange capacity have the problem of high water uptake, which can be solved by the cross linking. Sulfuric acid has been used as a cross linking agent for chitosan based membranes [25-26]. In this study, in order to improve the mechanical properties as well as proton conductivity, chitosan was doped with 5 – 15% of MSA and SDBS. The prepared membranes were cross-linked with 0.5M sulfuric acid solution in order to maintain hydrolytic stability of the membranes. To the best of our knowledge, the synergistic effect of dopant (MSA and/or SDBS) and cross linking agent has not been reported before. The membranes were characterized in detail by FTIR and UV-Visible spectroscopy, atomic force microscopy (AFM), mechanical properties, thermal and oxidative stability, ion exchange capacity, water and methanol uptake and proton conductivity at different temperatures as well as frequencies. The results are discussed in detail and compared with previously reported systems.

2. Experimental

2.1 Materials

Chitosan has molecular weight~ 2×10^5 and degree of deacetylation 90% was purchased from Acros organics. Acetic acid (99%) and sulfuric acid (98%) were supplied by Merck limited (Mumbai). Methane sulfonic acid (MSA) (99%) was procured from Merck Millipore India Pvt Ltd (Bangalore). Sodium salt of dodecylbenzene sulfonic acid (SDBS) was purchased from Sigma Aldrich. The entire reaction was carried out in de-ionized water. All the reagents were used as received without further purification.

2.2 Membrane preparation

Doped chitosan membranes (CS-MSA and CS-SDBS) were prepared by reacting chitosan acetate solution with MSA and SDBS. 1.5 g of chitosan powder was dissolved in 100 ml of 1% (v/v) acetic acid solution to form chitosan acetate solution. After complete dissolution of chitosan powder, methane

sulfonic acid (MSA) of 0, 5, 10 and 15wt% of chitosan was added individually to the chitosan acetate solution and mixed for about 4 h at room temperature. The solution was allowed to stand for 12 h at room temperature to remove air bubbles and then cast onto a clean glass petri dish and dried at room temperature for 48 h and the bubble free film was peeled off with the help of a sharp knife. The resultant dried membranes (film) were further subjected to cross linking through immersion in 0.5 M H_2SO_4 solution for 24 h at room temperature. The cross-linked films were then washed with deionized water to remove unreacted dopant and cross linking agent. The cross-linked films were further dried in a vacuum oven at ambient temperature for 24 h. The membranes thus obtained were designated as CS (neat chitosan), CS-MSA-5, CS-MSA-10 and CS-MSA-15 respectively. The samples were kept in desiccator in order to avoid exposure to moisture before further characterization. All membranes had a thickness of 50 – 100 μm. The similar procedure was also used in the case of chitosan doped with sodium salt of dodecylbenzene sulfonic acid (SDBS) based membranes (5, 10 and 15wt %) and designated as CS-SDBS-5, CS-SDBS-10 and CS-SDBS-15 respectively.

2.3 Membrane characterization

Fourier transform infrared spectroscopy (FTIR) studies were performed to find any possible interaction among different chemical groups present in doped and cross-linked chitosan. The Fourier transform infrared spectroscopy (FTIR) was done using Perkin Elmer FTIR spectrometer in the attenuated total reflectance (ATR) mode in the wavenumber region of 4000-650 cm^{-1}.The UV-Visible optical absorption spectra of the membranes were recorded over the wavelength region of 200 – 700 nm, with scan rate of 120 nm/min using Perkin Elmer UV - Win lab spectrometer by directly inserting the membrane in the beam. The surface topography and phase image of the membranes was investigated using an atomic force microscopy (AFM) (Agilent technologies 5500) in tapping mode. The roughness was obtained from the 5 μm × 5 μm scan. The surface and cross-sectional morphology of the membranes was characterized by using a field emission scanning electron microscope (FE-SEM Zeiss, Merlin, Gemini – 2, Japan) at a magnification of 10000. The operational voltage was set to 5 kV to protect the biopolymer based sample.

The ultimate tensile strength and percentage elongation at break were measured using Tinusolsen Universal Testing Machine (UTM) (model, H50KS, UK). The testing was performed according to the standard ASTM D 638-08. Dumb-bell shaped specimens of the samples were punched out using an ASTM 412 – B die from the cast films. Measurements of hydrated membranes were taken on samples

immediately removed from water after being soaked for 24 h at room temperature. The results reported are based on the average values of three specimens. The ion exchange capacity (IEC) of membranes was determined using acid-base titration method (ASTM D 2180) using sodium chloride as the exchange medium. The membrane in the form of H^+ ions was converted to the Na^+ form after immersing in 1M NaCl solution for 24 hours at room temperature. Released H^+ ions were titrated with 0.01M NaOH solution using phenolphthalein indicator. The IEC of membranes were calculated using the following equation and expressed as mmol per gram of dry membrane.

$$\text{IEC} = {(C_{NaOH} * V_{NaOH})}/{W_{Dry}}$$

Where C_{NaOH} (mol/L) and V_{NaOH} (ml) are concentration and volume of NaOH solution required for neutralization of the solution and W_{dry} is the weight of the dry membrane.

Membrane hydrolytic stability was measured using water and methanol uptake. The membranes were dried at 80 °C for 24h, weighed (W_{dry}) and immersed in deionized water at three different temperatures (room temperature (RT), 80°C, 100°C) and methanol (1M and 5M) at RT, 50°C and 80°C separately for 24 hours. After wiping the surface water, the samples were quickly weighed (W_{wet}) and water / methanol uptake was calculated using the following equation:

$$\text{Water/Methanol uptake} = {(W_{wet} - W_{Dry}) * 100}/{W_{Dry}}$$

The thermal stability of the prepared membranes was determined using thermogravimetric analyzer (TGA/DSC 1, Mettler Toledo) under nitrogen atmosphere from room temperature to 700°C at 20°C/min heating rate. The oxidative stability of the membranes was evaluated by recording the percentage weight loss in the membrane (2 × 2 cm^2) after being soaked in Fenton's reagent (3 % H_2O_2 with 2 ppm $FeSO_4$) at 80°C for 1h. The proton conductivity of polymer electrolyte membranes was measured using a high performance ac impedance analyzer (Win deta Novotherm α) over a frequency range of 1–10^6 Hz with the voltage of 10 mV. The membranes of 14 mm diameters and 0.05-0.07 mm thickness were sandwiched between two copper electrodes and kept in a thermal chamber. For conductivity measurements in the hydrated state, the membranes were immersed in de-ionized water at room temperature for 24 h. Before the measurement, the surface water was properly removed and the swollen

membrane was quickly placed in the measurement cell. The measurements were performed at temperature of 40 – 125 °C. The proton conductivity was calculated as follows:

$$\sigma = {}^{d}/_{(R_b * A)}$$

Where σ is conductivity (S/cm), d is the thickness of the sample (cm), R_b is the bulk resistance (Ω) and A is the area of sample (6.15 cm^2).

The prepared membranes were electrochemically characterized at room temperature using cyclic voltametry. The measurement set up consist of a typical cell with Ag/AgCl, platinum wire and the prepared membrane as reference, counter and working electrode respectively with the electrolyte of 1M H_2SO_4 solution. The cell was connected to an autolab N-302 potentiostat/galvanostat and the voltagrams were obtained by scanning at 20mV/sec from -0.2 to 6.0 V.

3. Results and discussion

3.1 Structure and morphology of membranes

FTIR spectra of pure chitosan powder, cross-linked CS-MSA and CS-SDBS membranes were recorded to investigate the interaction among different groups present in chitosan, dopants (MSA and SDBS) and cross linking agent (H_2SO_4). Fig. 1(a) shows the FTIR spectra of pure chitosan powder and undoped cross-linked chitosan film. The peak appeared at 1645 cm^{-1} in pure chitosan powder is associated with C=O stretching of secondary amide and the peak at 1156 cm^{-1} corresponds to C-O-C antisymmetric stretching, whereas the doublet peaks at 2926 and 2866 $cm^{-1}$are attributed to the C-H symmetrical and asymmetrical stretching respectively. The symmetric bending vibration of C-H and stretching of C-O are appeared at 1378 and 1080 cm^{-1}respectively [25,27-30]. After cross-linking with H_2SO_4, definite changes are observed in the FTIR spectrum of pure chitosan. Based on the spectral information, the schematic route for different interactions is described in Fig. 2. The spectrum of pure chitosan powder shows the strong characteristic absorption band in between 3000 cm^{-1} and 3700 cm^{-1}, which is ascribed to the stretching vibration of N-H (primary amine) and O-H groups exhibit strong hydrogen interactions [25,29]. After cross linking with sulfuric acid, this band became broader and shifted to the lower wavenumber region attributed to the protonation of NH_2 group and hence changes in hydrogen bond structure. In addition, the absorption peak at 1156 cm^{-1} attributed to C-O-C stretching is obscured by broad band at 1017 cm^{-1} after cross linking. The appearance of two new peaks at 1533 cm^{-1}

and 699 cm^{-1} are due to the symmetric bending vibration of NH_3^+ and S-O deformation respectively after cross linking reveals the existence of strong ionic interaction between negatively charged SO_4^{2-} ions of cross linking agent (sulfuric acid) with the positively charged amino groups in chitosan (Fig. 2a) [11,25,31]. The absorption band at 1645 cm^{-1} shifted to 1630 cm^{-1} which again reveals the formation of hydrogen bonding between acetamide and sulfuric acid (Fig. 2b). The preparation of membranes through cross linking of chitosan or its blends with sulfuric acid and their spectral characteristics were reported earlier in the literature [12,25]. Our results are in good agreement with published literature and support the conclusion of formation of electrostatic interactions between sulfate anion and protonated amino group and / or acetamide group of chitosan. The formation of cross links among chitosan polymer chain through H_2SO_4 was also confirmed by solubility characteristics of membranes before and after cross linking, when it is immersed in water for 24 h. Before cross linking, the membrane was readily dissolved, but after cross-linking instead, swelled which confirms the cross-linked structure formed in the membranes.

Fig. 1 (b and c) displays the IR spectra of doped chitosan membranes by MSA and SDBS with varying concentration of 0 wt% to 15 wt% respectively. In the IR spectra of MSA and SDBS doped membranes, peaks due to all expected functional groups of chitosan backbone structure are observed. However after the addition of dopants, the peak at 1645 cm^{-1} of pure chitosan powder (Fig. 1a) shifted to the lower wavenumber and a new peak with increase in intensity with dopant concentration is observed at 1533 cm^{-1} (symmetric N-H deformation in protonated amine) in both MSA and SDBS doped membranes [12]. Moreover, the sharp increase in intensity of peak at around 1020 cm^{-1} with increase in dopant concentration observed is due to the overlapping of C-O stretch in primary alcohol of chitosan and S=O stretch (1024 cm^{-1}) in sulfonic acid (MSA and SDBS), which confirms the presence of $-SO_3H$ group in doped membranes [5,32]. The increase in the intensity of the peak at 2359 cm^{-1} indicates the presence of O-H stretching vibration in SO_3H. The appearance of the peak due to $NH_3^+$and S=O at 1533 cm^{-1} and 1024 cm^{-1} indicate the evidence of successful doping of MSA and SDBS into chitosan matrix possibly through ionic bonding between NH_2 and SO_3groups (Fig. 2c). The shift in peak due to C=O group of amide II linkage is observed due to the hydrogen bonding between amide and sulfonic groups (Fig. 2g). Further, the sharpening of the band between 3000 cm^{-1} and 3700 $cm^{-1}$and increase in the intensity of the peak at around 1020 cm^{-1} after MSA and SDBS doping in membranes confirms the formation of hydrogen bond among hydroxyl, amine and sulfonic groups of the matrix and dopants (Fig. 2d - f) [33-36].

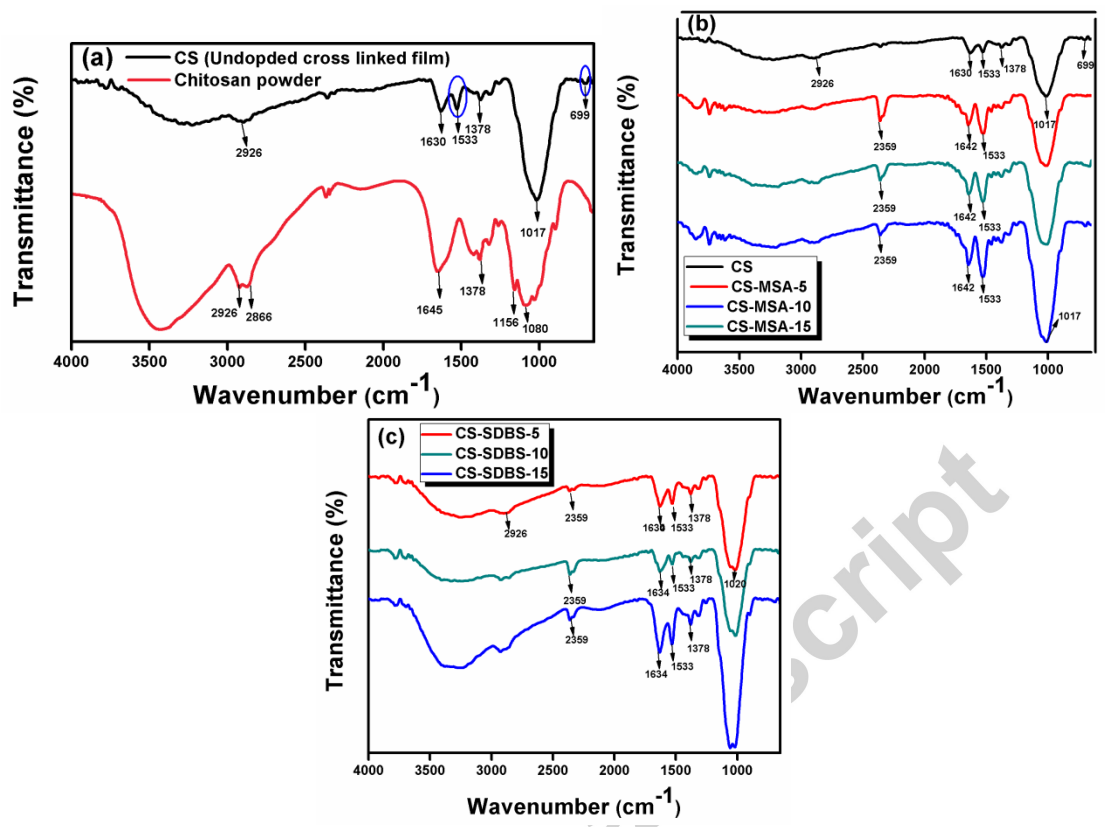

.**Fig. 1** FTIR spectra of (a) Chitosan powder and undoped cross-linked chitosan membrane (CS) (b) CS-MSA and (c) CS-SDBS membranes

The physico-chemical interactions between chitosan and its dopants in CS-MSA and CS-SDBS membranes were confirmed by UV-visible spectroscopy. Fig. 3 shows the absorption spectra of CS-MSA and CS-SDBS membranes in the range of 200 – 700 nm. Obviously, the uncross-linked chitosan membrane exhibited characteristics peaks centered at circa 253 nm and 310 nm. These are attributed to n – π^* and n - σ^* transitions of C=O and NH_2 groups respectively. After incorporation of different concentrations of dopant (MSA or SDBS) and cross linking agent, the peak at 253 nm disappeared, and absorption band at around 310 nm shifted towards lower wave number. In the presence of dopant and cross- linking agent the positively charged amino groups are ionically bonded with SO_3^- (Fig. 2c) and SO_4^{2-} (Fig. 2a) groups respectively, which donates nitrogen with stream of electrons and decreases the energy level of σ^*. As a result, a blue shift of transition from 310 nm (uncross linked membrane) to 306 nm (doped and cross-linked membranes) has been observed [37]. Furthermore, the disappearance of hump at 253 nm in doped and cross-linked membranes demonstrates the existence of electrostatic interaction among acetamide and sulfuric acid (Fig. 2b) or sulfonic group (Fig. 2g) of chitosan, cross-

linking agent and dopants. The similar spectral pattern observed for all the membranes, which suggests that these membranes are well doped with sulfonic acid (MSA and SDBS). These observations are in good agreement with the results obtained by FTIR analysis. All the membranes are clear and transparent.

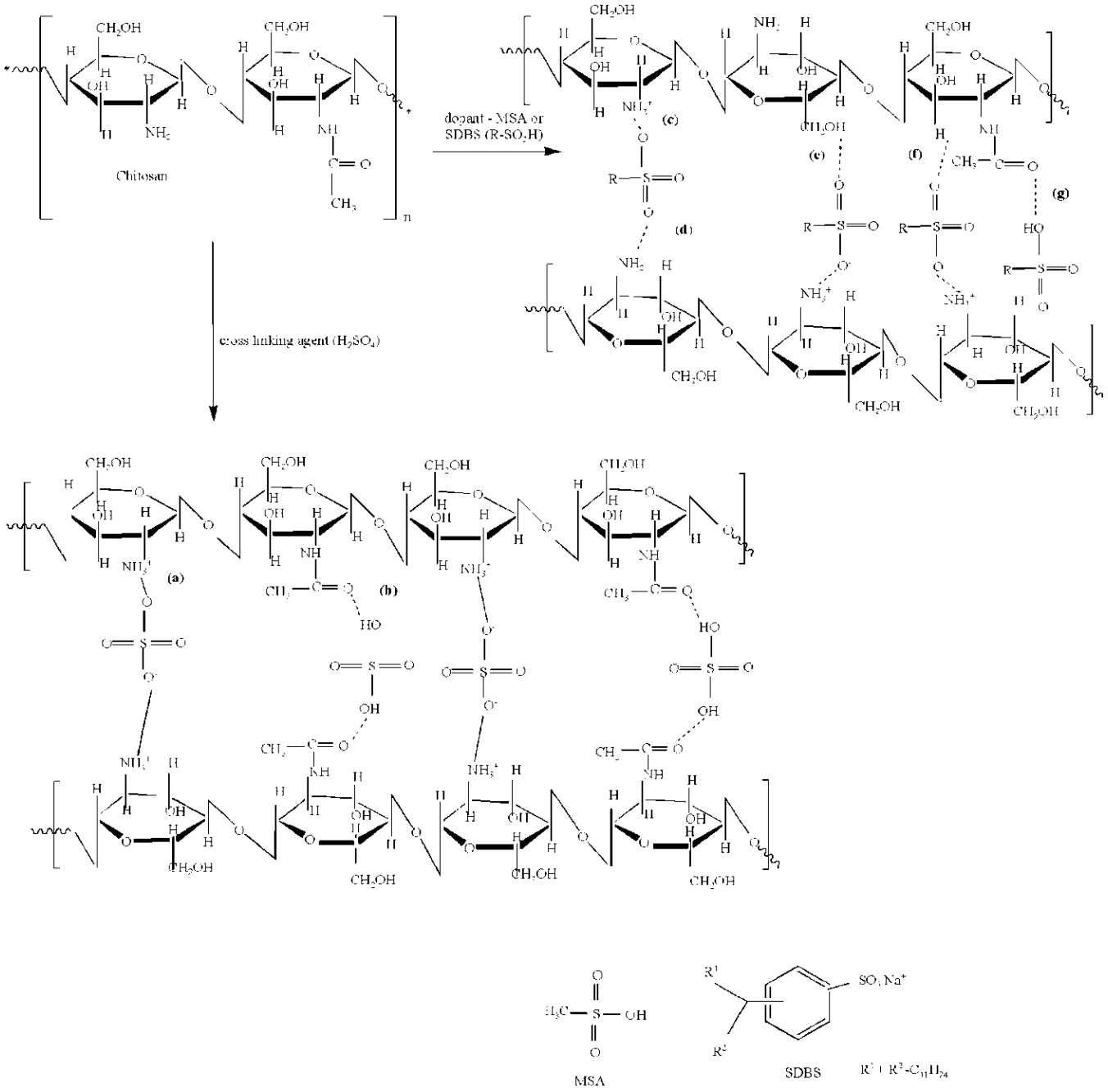

Fig. 2 A pictorial representation of both doped and cross-linked membrane.

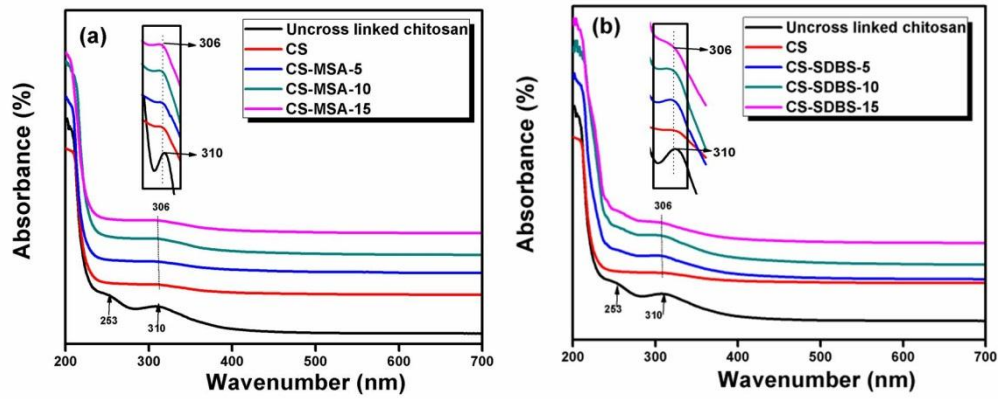

Fig. 3 UV-Visible absorption spectra of (a) CS-MSA and (b) CS-SDBS membranes

Atomic force microscope (AFM) was employed to investigate the surface morphology evaluation of chitosan membranes after doping with MSA and SDBS. The AFM topographical images of the MSA and SDBS doped CS membranes were recorded using tapping mode under ambient conditions, as presented in Fig. 4 (a – g). The dark areas and the bright areas in AFM phase images are ascribed to the hydrophilic (ionic) and hydrophobic domains respectively. The CS membrane shows a homogeneous, dense and smooth surface. However, with increase in MSA and SDBS content, more dark area observed indicates the increase in hydrophilic structure of the membranes. Table 1 reports the quantitative data on surface roughness in terms of root mean square value for surface roughness. The mean roughness of the surface topography of the membranes was found to increase from 4.66 nm to 7.55 nm and 17.4 nm respectively with increase in MSA and SDBS dopant content from 0 to 15 wt% respectively. Comparatively higher roughness has observed for CS-SDBS membranes, which is due to presence of rigid aromatic structure of SDBS. The variation in surface structure follows the trend of water uptake. Thus the increase in hydrophilic domains with increasing MSA and SDBS content contributed towards higher hydrophilicity of the membranes.

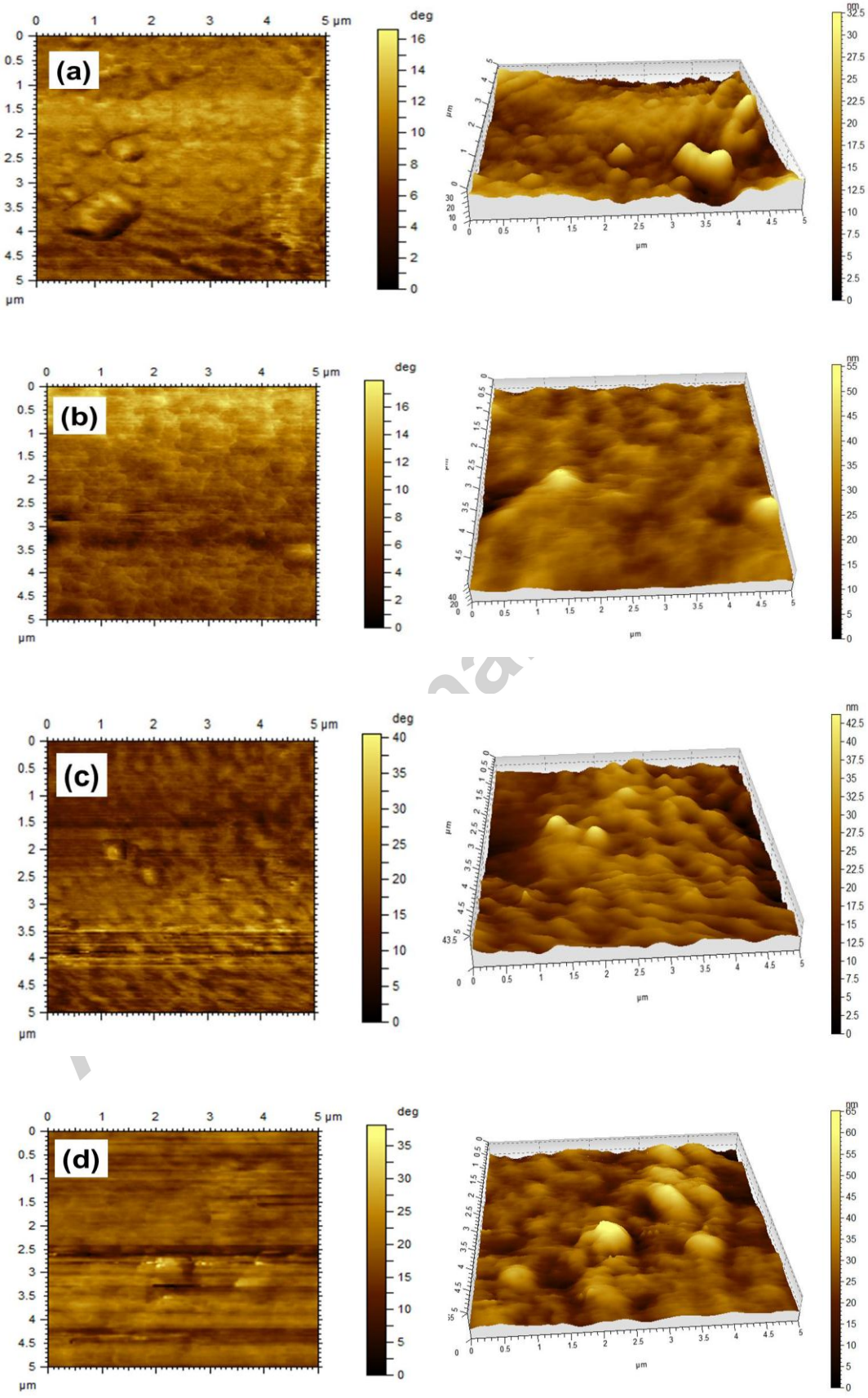
(a)
(b)
(c)
(d)
deg
nm
µm

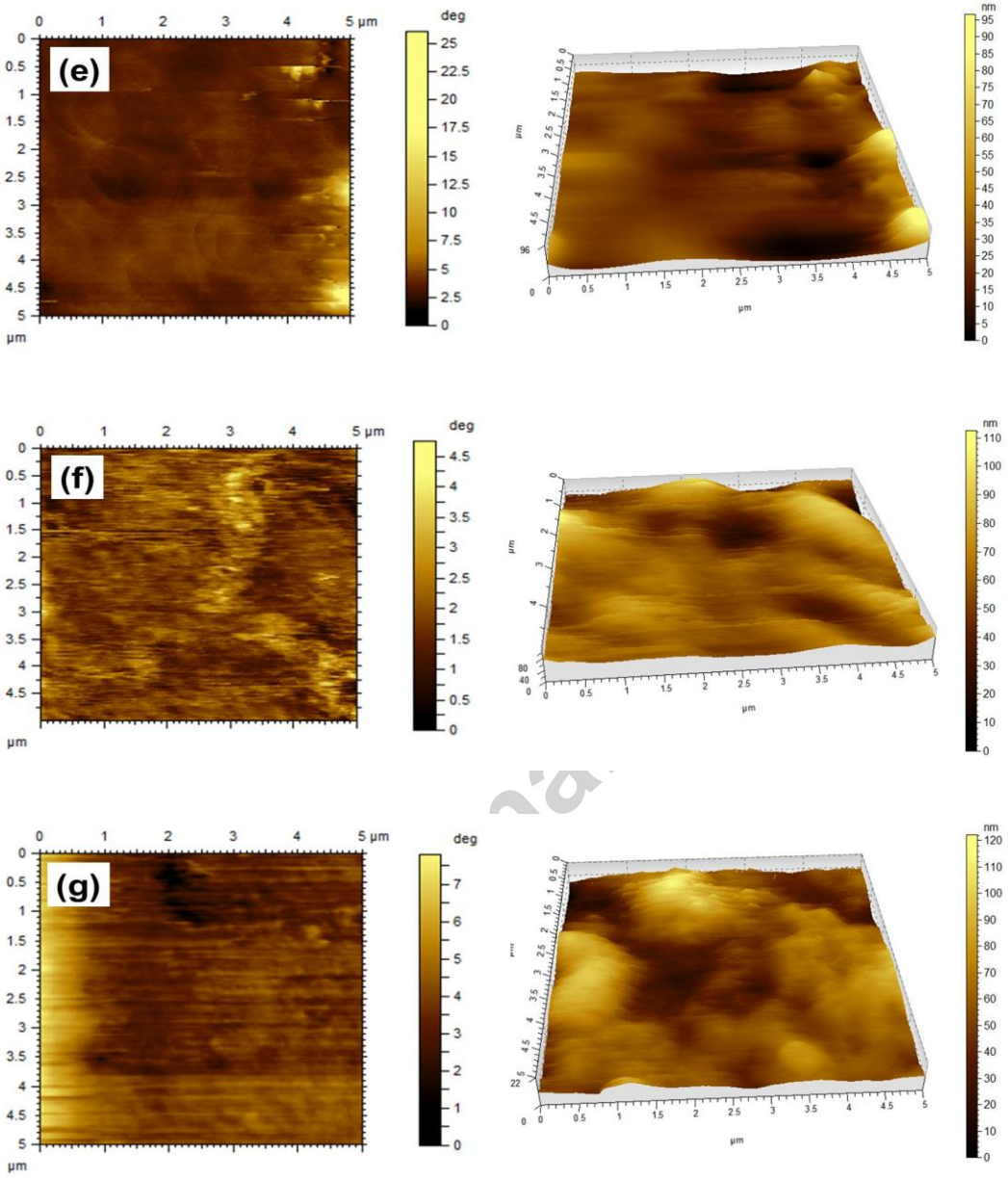

Fig. 4 Phase and topographical images of (a) CS (b) CS-MSA-5 (c) CS-MSA-10 (d) CS-MSA-15 (e) CS-SDBS-5 (f) CS-SDBS-10 (g) CS-SDBS-15

The surface and cross- sectional (tensile fractured surface) morphology of chitosan membranes with various dopant (MSA and SDBS) concentration are shown in Fig. 5 (a – g). The membranes show homogeneous and non – porous structure in the morphology without obvious phase separation or cracks. This indicates the good compatibility between chitosan and dopants (MSA and SDBS) in the membranes. The proton conductivity of the membranes is the result of a complex process dominated by the surface and chemical properties of both chitosan and dopants [12]. From the micrographs, it can be

seen clearly that surface morphology of the membranes after doping becomes rougher compared to that of pristine chitosan membrane. The roughness is more in CS-SDBS membranes than CS-MSA membranes, which support the AFM data. The submicron particles of SDBS became increasingly visible with increasing content of SDBS in the membrane. The increase in surface roughness in both MSA and SDBS doped membranes confirm its higher hydrophilicity, which helps in water absorption and hence dissociation of sulfonic acid and proton conduction.

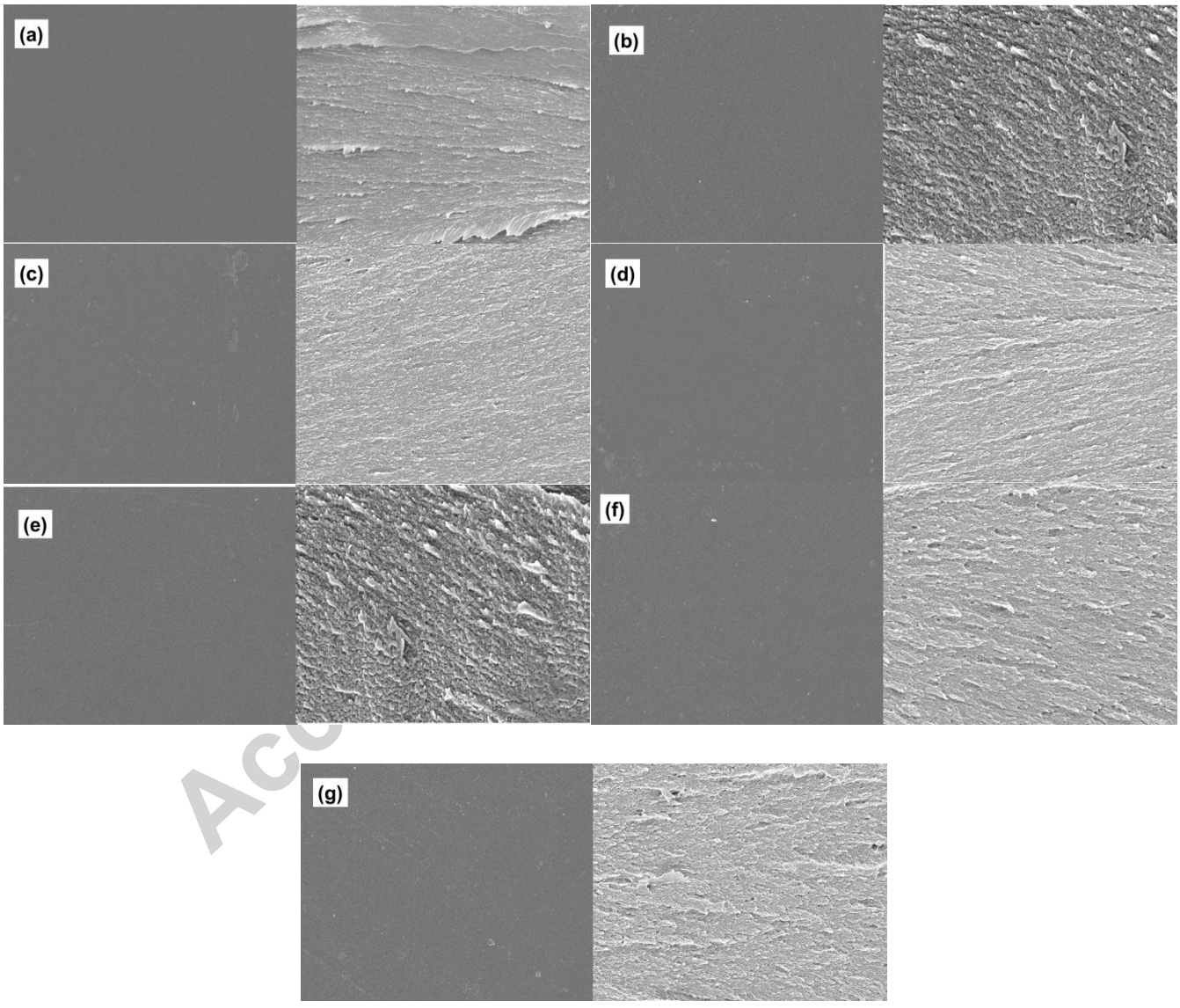

Fig. 5 Surface and cross – sectional SEM images of (a) CS (b) CS-MSA-5 (c) CS-MSA-10 (d) CS-MSA-15 (e) CS-SDBS-5 (f) CS-SDBS-10 (g) CS-SDBS-15

3.2 Solvent uptake and stability studies

Water and methanol uptakes are two important parameters to be considered for ion transport and fuel crossover for proton exchange membranes (PEMs) used in direct methanol fuel cells. It is generally accepted that the water uptake property has a profound influence on both mechanical stability and proton conductivity of the polymer electrolyte membranes. The presence of water molecules in the membrane matrix facilitates the dissociation of functional groups required for high proton conductivity. However, an excessive water uptake in PEM leads to unacceptable dimensional change when used in fuel cell assembly [38]. The water and methanol uptake for different membranes were measured, and relevant data in the form of bar charts and plots are presented in Fig. 6 (a-e). The functional and hydrophilic characteristics of the membranes were significantly increased with MSA and SDBS content which is attributed to the increase in charge density due to the presence of sulfonic acid group. The water uptake of pristine chitosan membrane (CS) at room temperature was 38.5%, but as the doping level of MSA and SDBS increase the water uptake is also increased. The maximum of 88.5% and 71.4% water uptakes were observed at room temperature for CS-MSA-15 and CS-SDBS-15 membranes respectively. The presence of increased number of functional group (-SO_3H) increases hydrogen bonding through water molecules accommodated in the space between adjacent polymer chains leading to higher water uptake in the doped membranes [39]. In CS-SDBS membranes, the presence of aromatic rings in SDBS makes the polymer structure strong however, its lower number of functional group (-SO_3H) reduces water uptake compared to MSA doped membranes.

Besides water uptake characteristics, methanol uptake is also another important property to determine the quality of PEM, especially for direct methanol fuel cell (DMFC) applications. Less methanol uptake is necessary for a PEM to reduce the fuel loss and increase the efficiency of DMFC. CS-MSA and CS-SDBS membranes exhibit low methanol uptake compared to water uptake and the value decreases with increase in methanol concentration, which reveals the higher water uptake, but lower methanol selectivity of these membranes. It is observed from the Fig. 6c that the methanol uptake of CS-MSA membranes was lower than that of CS-SDBS membranes, which may be due to the reduction in inter chain space in the presence of MSA compared to SDBS [40].

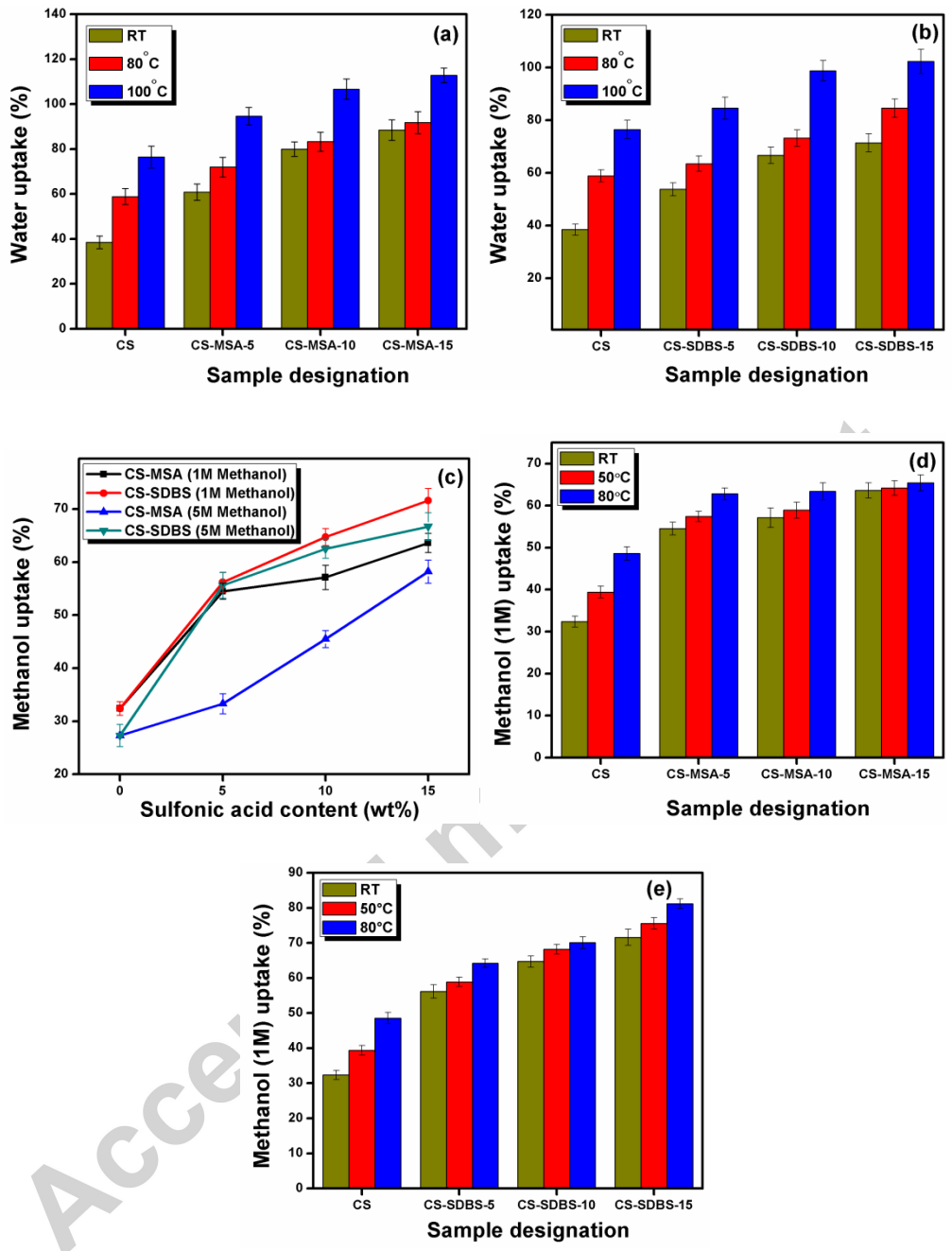

Fig. 6 Water uptake of (a) CS-MSA and (b) CS-SDBS membranes at three different temperatures, (c) comparison of methanol uptake in CS-MSA and CS- SDBS membranes at RT, methanol uptake of (d) CS-MSA and (e) CS-SDBS membranes at three different temperatures

The effect of temperature on solvent uptake ability of the prepared membranes was performed to study its performance at elevated temperatures, water and methanol (1M) uptake of all the membranes increased with temperature (Fig. 6d-e). This variation was attributed to the increased chain motion due

to thermal excitation and hence increases in free volume and easy penetration of the solvent molecule into the swelled polymer matrix. The water and methanol uptake of the developed membranes at room temperature were similar to that of Nafion-117 membrane reported elsewhere [38,41].

3.3 Ion Exchange Capacity (IEC)

Ion exchange capacity (IEC) is the key parameter for the performance of a proton exchange membrane and mainly depends upon the population of ionizable hydrophilic functionalities present in the polymer matrix and hence is responsible for proton conduction. Table 1 presents the IEC values of the MSA and SDBS doped membranes. IEC values of the membranes increase with increase in the content of MSA and SDBS resulting in increased concentration of more H^+ ions attached to the material. These protons are pushing other cations from the system into the membrane – water solution thereby increasing the cation exchange capacity [14]. The highest IEC value was found to be 0.35 mmol/g, observed for the CS-MSA-15 membrane. The sulfonic acid groups provide channels inside the polymer matrix thereby making the membrane more hydrophilic in nature, which in turn provides the passage of counter ion through the membrane resulting in a gradual increase of proton conduction. This is reflected in Fig. 5 (a – b), when water uptake increases with the amount of dopant used and ion exchange capacity increases with water uptake capacity.

Table. 1 RMS roughness and IEC of CS-MSA and CS-SDBS membranes

Sample designation	CS	CS-MSA-5	CS-MSA-10	CS-MSA-15	CS-SDBS-5	CS-SDBS-10	CS-SDBS-15
rms roughness (nm)	4.66	4.94	5.84	7.55	10.6	12.9	17.4
IEC (mmol/g)	0.16	0.28	0.31	0.35	0.19	0.24	0.27

3.4 Mechanical properties

Adequate mechanical strength is required for handling of these membranes. The mechanical property of membrane affects the durability of a membrane electrode assembly of a PEMFC [11]. Good mechanical properties of polymer electrolyte membranes in anhydrous and hydrous states are one of the necessary demands for their practical applications. In a literature, it was reported that chitosan

membrane cross-linked with 0.5M H_2SO_4 possesses the high conductivity and good mechanical properties [40]. The same idea was therefore used to prepare membranes containing various dosages of MSA and SDBS as dopants. The mechanical stability of CS-MSA and CS-SDBS membranes in dry and hydrated states were measured in terms of tensile strength and elongation at break and shown in Fig. 7. In comparison with the pristine CS membrane, all doped membranes exhibit significantly increase in tensile strength both in dry and hydrated states because of the enhanced coulombic interaction between sulfonic acid groups of dopants and amine group of chitosan. In addition, the hydroxyl group of chitosan can also form hydrogen bonding with $–SO_3H$ groups of dopant and these electrostatic interactions can enforce some restriction in the polymer chain mobility as a result an increase in tensile strength and decrease in elongation at break of the membranes are observed. With increase in dopant concentration, the concentration of interacting groups increases, and strength of membranes increases with decrease in elongation at break. However, comparatively more number of reactive $–SO_3H$ sites on weight base are present in CS-MSA membrane compared to that of CS-SDBS membrane, as a result CS-MSA membrane exhibit higher tensile strength than that of CS-SDBS membranes. It is worth mentioning here, the tensile strength of CS-MSA and CS-SDBS membranes exhibit higher tensile strength compared to standard Nafion membrane (23.6MPa) even at 5 wt% loading [12].

However, all membranes exhibit less tensile strength, but the increase in elongation at break in hydrated state compared to the dry state. This may be due to ion dissociation effect in hydrated state i.e., $SO_3^-…NH_3^+$ interaction weakens in the presence of water (H-OH). The presence of free ions facilitates the separation of polymer backbone and may result in the decreasing intermolecular force and low tensile strength in hydrated conditions [10,39]. The tensile results in both the dry and hydrated states undoubtedly showed the prepared membranes are quite strong and adequately flexible material. Thus CS-MSA and CS-SDBS membranes have enough flexibility and mechanical strength requirement to be appropriate proton exchange membrane for fuel cell application.

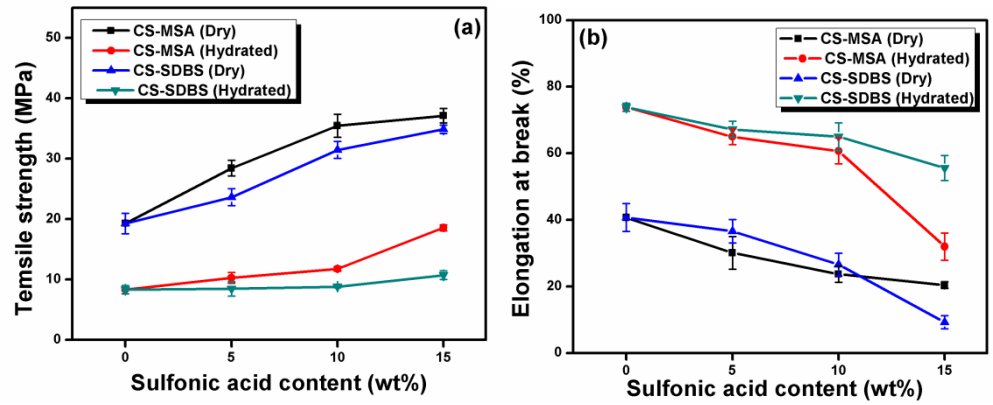

Fig. 7 (a) Tensile strength and (b) Elongation at break of CS-MSA and CS-SDBS membranes in dry and hydrated states

3.5 Thermal and oxidative stability

The thermal stability of doped chitosan membranes with various amounts of MSA and SDBS and blank sample (uncross-linked chitosan membrane) was analyzed by TGA as presented in Fig. 8. The blank sample is prepared in the same way as CS membrane, without doping and cross linking. The TGA result of the blank sample shows only two stages of decomposition. However the CS-MSA and CS-SDBS membranes exhibit three stages of decomposition. The initial weight loss within 60 - 150°C is attributed to the loss of moisture content and weakly bonded solvent molecules with the membranes [14] while the second stage weight loss (200 - 260°C) is considered to be due to the decomposition of oxygen containing functional groups such as sulfonic acid (from dopant) and sulfuric acid (cross-linker) present in the membranes [7,16,42]. The absence of the second stage of decomposition in the blank sample confirms the formation of doped and cross-linked structure in CS-MSA and CS-SDBS membranes. The third stage of weight loss (260 - 500 °C) is due to the degradation of chitosan backbone chains [15]. The major thermal degradation step within 260 - 400°C does not change much with increased addition of sulfonic acid. In fact, both doped membranes CS-MSA and CS-SDBS exhibit good thermal stability similar to that of undoped CS membrane.

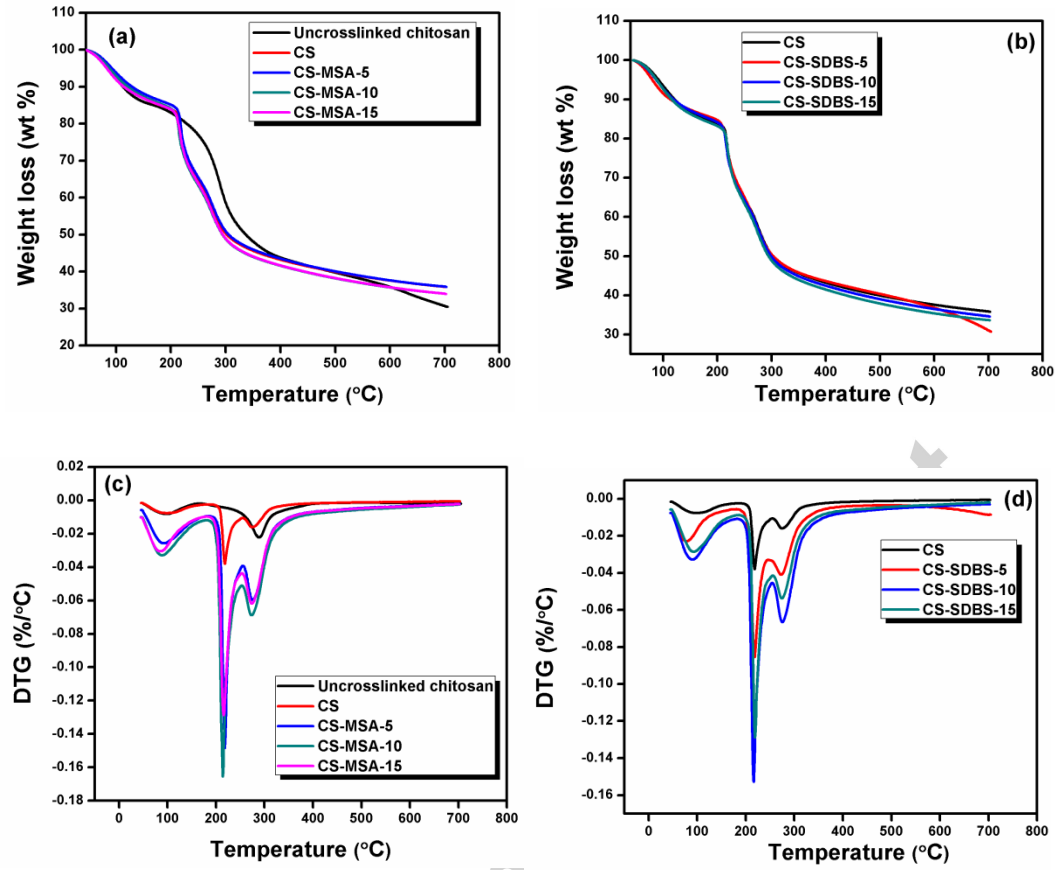

Fig. 8 TGA curves of (a) CS-MSA (b) CS-SDBS and DTG of (c) CS-MSA (d) CS-SDBS membranes

From the TGA and DTG curves, onset temperatures for different stages of decomposition, final residue in weight %, and weight loss (%) at each step of degradation are calculated and summarized in Table 2. A complete weight loss is not attained for the prepared membranes even after heating the material up to 700°C [43]. All the doped membranes show a residual mass of more than 30 wt% on pyrolysis under nitrogen atmosphere indicates the presence of non-volatile carbonaceous elements present in the base polymer. Due to doping with MSA and SDBS, there is only marginal improvement of thermal stability of neat CS membranes as revealed from plots and table. However it is well above the desirable fuel cell operation temperature (≤ 100°C) [44].

To evaluate whether the membranes could withstand the oxidative environment during fuel cell operation, the oxidative stability was evaluated by immersing the film in Fenton's reagent at 80°C for 1h. The most common degradation mechanism described in the literatures is the attack of polymer chain by hydroxyl ($OH^{\cdot}$) and hydroperoxyl ($HOO^{\cdot}$) radicals formed in situ during operation. This leads to the reduction of membrane weight due to break down of polymer backbone into small pieces, followed by

dissolution in Fenton's reagent [39-40,45]. All the developed membranes were found to be in an original unbroken state with loss of about 2.05 – 3.52 % (Table 2) after oxidative experiment revealing enough stability even after doping. In SDBS doped membranes the presence of benzene ring in its structure improves its oxidative stability compared to CS-MSA membranes.

Table 2 TGA and oxidative stability results of chitosan membranes

Sample designation	Onset temperature of degradation (°C)			Weight loss (%)			Residue at 700° C (wt%)	Oxidative stability (wt% loss)
	First	Second	Third	First	Second	Third		
Uncrosslinked chitosan	97.48	287.09	-	7.02	34.95	-	30.71	-
CS	101.69	217.91	275.47	6.8	21.3	42.69	35.87	2.05
CS- MSA-5	91.37	217.75	275.63	4.81	20.31	41.92	35.76	2.62
CS- MSA-10	89.04	215.59	274.05	5.29	23.29	43.85	34.03	3.10
CS- MSA-15	81.64	220.57	275.59	5.51	24.09	43.72	34.02	3.52
CS-SDBS-5	76.82	217.82	276.48	4.13	21.66	43.50	31.04	2.51
CS-SDBS-10	91.63	217.92	275.04	5.78	23.36	43.01	34.64	2.92
CS-SDBS-15	91.22	220.47	276.45	5.64	24.28	44.69	33.66	3.43

3.6 Proton conductivity

The proton conductivity of the CS-MSA and CS-SDBS membranes in the dry and hydrated state were plotted as a function of temperature as shown in Fig. 9. The linear increase in conductivity with temperature observed for all the membranes, which confirms the Arrhenius mechanism of conduction, that is, Grothus/hopping of conducting species, most likely H^+ ions, between SO_3^- groups and also NH_3^+. It has been suggested that, due to the electrostatic interaction among chitosan, MSA/SDBS, and sulfuric acid, resulting in numerous hydroxyl ions OH^-, H^+, $-NH_3^+$ and heteropolyanions, the proton can transfer along the ionic and hydrogen bonds through hopping from one functional group to the another [39].

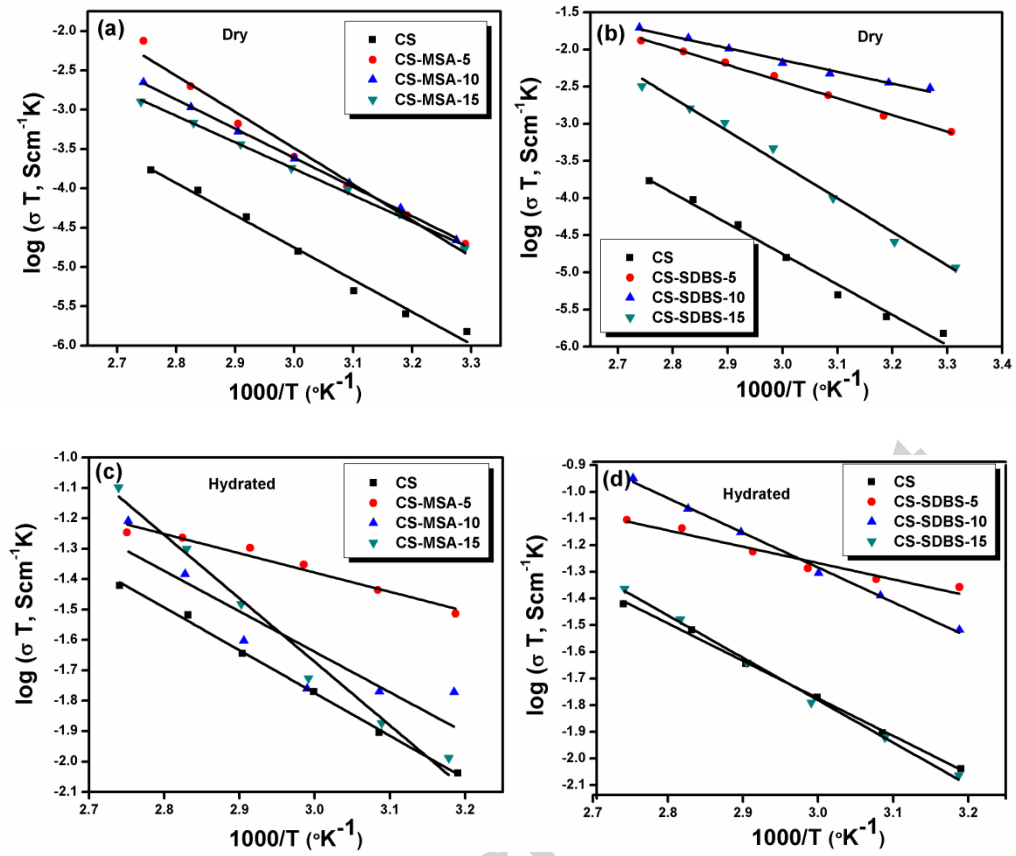

Fig. 9 Arrhenius plot of ionic conductivity of (a) CS-MSA (dry) (b) CS-SDBS (dry) (c) CS-MSA (Hydrated) (d) CS-SDBS (Hydrated) membranes

The conductive performance of a polymer electrolyte membrane is closely related to its degree of hydration [7,27]. After hydration, the proton conductivity of the membranes was found to be higher than that in the dry state due to the higher ionic concentration resulting fron dissociation of ionic groups like sulfonic acid, as water has high dielectric constant (~ 80) helps in dissociation. The maximum proton conductivity observed for CS membrane was 1.04×10^{-4} S/cm at 363°K. It is noteworthy that the CS-SDBS-10 (3.09×10^{-4} S/cm) and CS-MSA-15 (2.18×10^{-4}S/cm) membranes show higher proton conductivity. The presence of benzene ring in SDBS prevents ion cluster formation because of its rigid structure, and this helps in ionic conductivity, as ion cluster formation hampers ionic mobility [21]. Hydrophilic hydrogen bonding ($SO_3\ldots H_2O$) facilitates the proton transport in hydrated membranes. In addition, due to high water uptake, continuous hydrophilic channels can form through chitosan, dopants and cross-linking agent which facilitates the proton transfer through vehicular mechanism in the form of hydronium ions. Therefore this study suggests that both vehicular and Grotthuss mechanism are

responsible for proton conductivity of the doped CS membranes. At higher concentration, the association of ion leads to cluster formation and thus there is decrease in the number of charge carriers and their mobility resulting in to decrease in ionic conductivity [46].

The activation energy is the minimum energy required for proton transport, and low activation energy can reduce the energy loss caused by the ionic resistance of the membranes [39]. From the plot of log (σ T) versus 1/T, the activation energy was calculated from the slope using the Arrhenius equation:

$$\sigma = (\sigma_0 / T) \exp (- E_a / RT)$$

Where Ea- activation energy for ionic conduction, σ_0- pre-exponential factor, T - absolute temperature and R-universal gas constant [47-48].

Table 4 shows the activation energy of CS-MSA and CS-SDBS membranes in dry and hydrated condition. In the hydrated state, there is an increase in the density of ions and hence decrease in energy barrier to the proton transport leads to the decrease in activation energy [47]. These activation energy values are comparable with those reported earlier. It is noteworthy that the activation energy (Ea) of conduction for CS-MSA-5 and CS-SDBS-5 membranes are quite low and values are comparable to that of Nafion – 117 membrane for which Ea value is 5.45 KJ/mol [38].

Table 4 Activation energy of different membranes

Sample designation		CS	CS-MSA-5	CS-MSA-10	CS-MSA-15	CS-SDBS-5	CS-SDBS-10	CS-SDBS-15
Ea (KJ/mol)	Dry	34.10	38.20	30.80	27.4	18.70	13.20	37.60
	Hydrated	11.60	5.24	11.10	17.30	5.09	10.80	13.20

The effect of frequency on conductivity of CS, CS-MSA-15 and CS-SDBS-10 membranes in hydrated state at different temperatures are illustrated in Fig. 10. From the figure, it can be observed that the conductivity of hydrated membranes gradually increases with increase in frequency up to around 10^4 Hz followed by sharp increase up to 10^6 Hz especially at high temperatures.

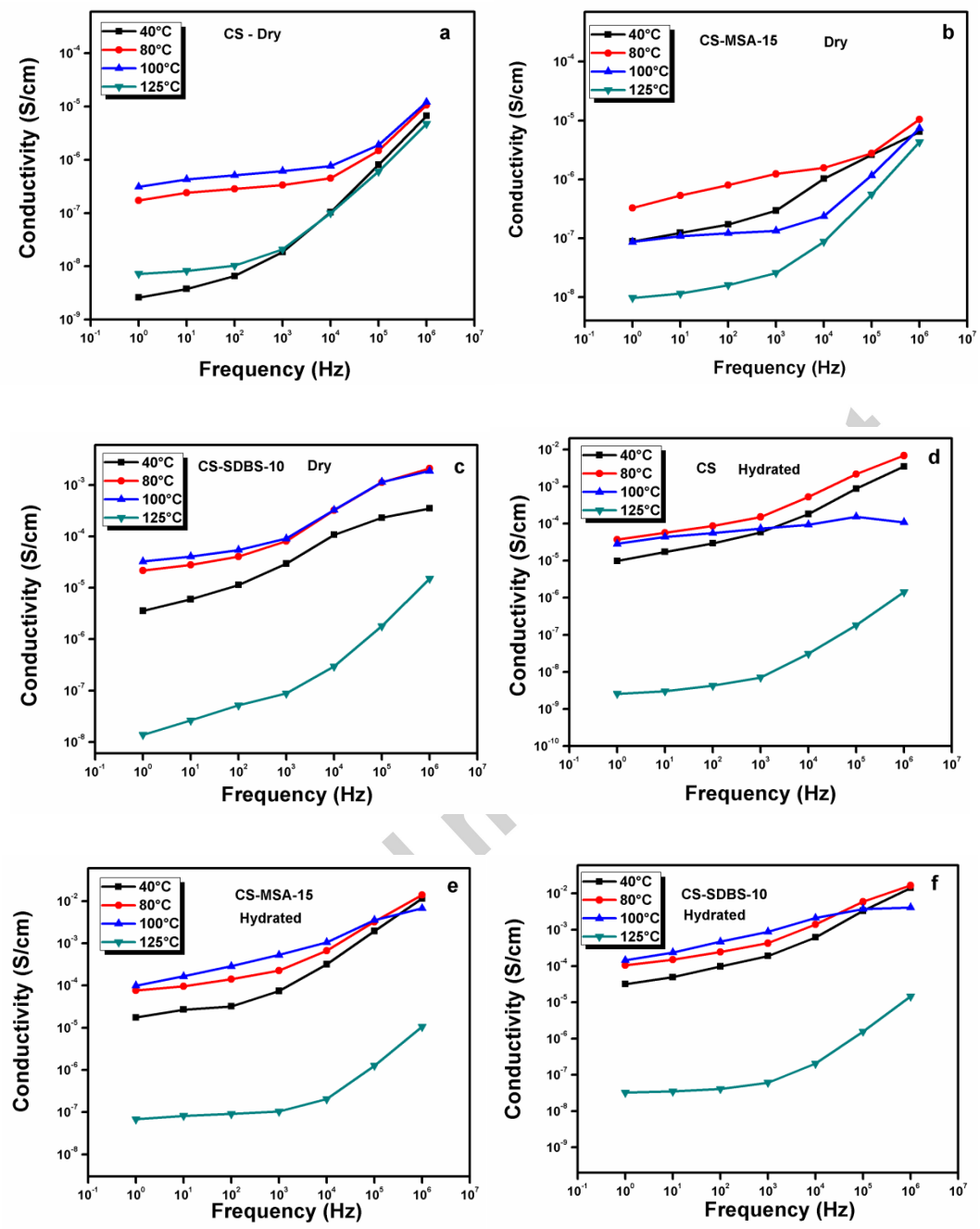

Fig. 10 Frequency versus ionic conductivity of (a) CS (b) CS-MSA-15 (c) CS-SDBS-10 in dry state and (d) CS (e) CS-MSA-15 (f) CS-SDBS-10 membranes in hydrated state at various temperatures

The high conductivity value at high frequencies are mainly due to the fact $\sigma_{AC} = \sigma_{DC} + 2\pi f\varepsilon''$ where, σ_{AC} is the conductivity under alternating field, σ_{DC} (under steady state potential) is mainly due to ionic conductivity and the second part $2\pi f\varepsilon''$ is mainly due to polarization process that is, restricted movement of bound charges like dipoles, (the present systems are highly polar). The contribution of second part

increases with increase in frequency till there is time lag between dipolar movement and reversal of alternating electric field. The CS doped with MSA and SDBS increases the conductivity and operating temperature range up to 100°C than neat CS membrane (undoped) whose maximum useable temperature limit is 80°C. The best conductivity results were obtained for CS-MSA-15 (2.86×10^{-4} S/cm) and CS-SDBS-10 (4.67×10^{-4} S/cm). As the temperature increases up to 100°C, the degree of ionic dissociation and re-association of the ion to aggregates increases resulting in the increased number of free ions or charge carrier concentration in the system and hence there is an increase in conductivity [15].

The Nyquist plots (real and imaginary components of complex impedance) of CS, CS-MSA-15 and CS-SDBS-10 membranes under hydrated state in the frequency range of 1 – 10^6 Hz at various temperatures are presented in Fig. 11 (a-c). High frequency is shown at the left of the Nyquist plot and the low frequency is towards the right. The impedance response of all the prepared membranes exhibits an incomplete semi-circle like curve indicating that the charge transfer mechanism involves both resistance and capacitance effects. According to literature, semicircle – like impedance response can be simulated by an equivalent circuit consisting ideally of parallel combination of resistance and capacitance arrangement. In this study, the ZSimpwin software was used to fit the experimental data to theoretically derived equivalent circuit model. Fig. 11 (d) shows the equivalent circuit and parameters after data fit in the circuit are given in Table 5. In the circuit, R_B is the bulk resistance of the membrane, R_A the charge transfer resistance at electrode interface and CPE (constant phase element), which is associated with surface roughness of the membranes or non-uniform current distribution. The behavior of the Nyquist plot obtained is in good agreement with that of SPEEK membrane reported by Mondel et al [49]. From the Table 5, it is observed that R_B value decreases with increase in temperature, which indicates increase in conductivity with temperature (Fig. 10 d-f).

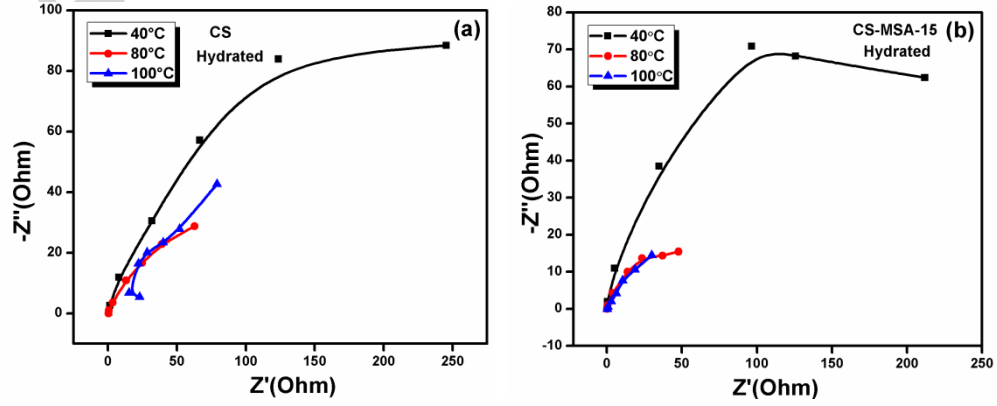

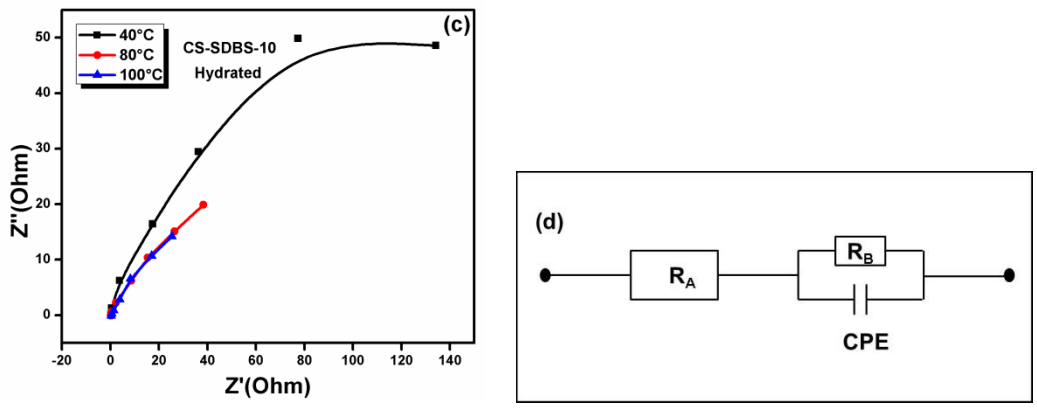

Fig. 11 Nyquist plots of (a) CS (b) CS-MSA-15 (c) CS-SDBS-10 in hydrated state at various temperatures and (d) equivalent circuit model

Table 5 Extracted parameters by fitting the impedance data to the equivalent circuit for different compositions at various temperatures

Sample designation	Temperature (°C)	R_A (Ω)	CPE (F)	R_B (Ω)
CS	40	8.6	4.09×10^{-7}	169.6
	80	30.64	1.10×10^{-6}	45.78
	100	22.94	1.58×10^{-6}	49.11
CS-MSA-15	40	1.76	1.48×10^{-7}	155.8
	80	3.21	1.0×10^{-6}	34.21
	100	3.62	8.83×10^{-6}	21.13
CS-SDBS-10	40	4.61	7.7×10^{-7}	95.85
	80	2.05	1.81×10^{-6}	29.30
	100	2.07	1.23×10^{-5}	20.46

3.7 Cyclic voltammetry

Cyclic voltammetry was used for analyzing the current – voltage response of the prepared membranes. Good electrical resistance is one of the necessary demands for the membranes to be used in

PEMFC applications. Fig. 12 presents the current - voltage (I-V) hysteresis curves of the prepared membranes at a scan rate of 20mV/sec over the potential range from -0.2 to 6.0 V. The very linear increase in current with applied voltage with very low hysteresis in the voltagram indicates the ohmic nature of the CS-MSA and CS-SDBS membranes. It is observed that the current density of the membranes decreases with increase in the content of MSA and SDBS up to 10 and 5 wt % loading respectively. The current density generally reflects the energy storage ability of the system; [50] the lower energy storage ability observed indicate the better electrical resistance of membranes under an electric field.

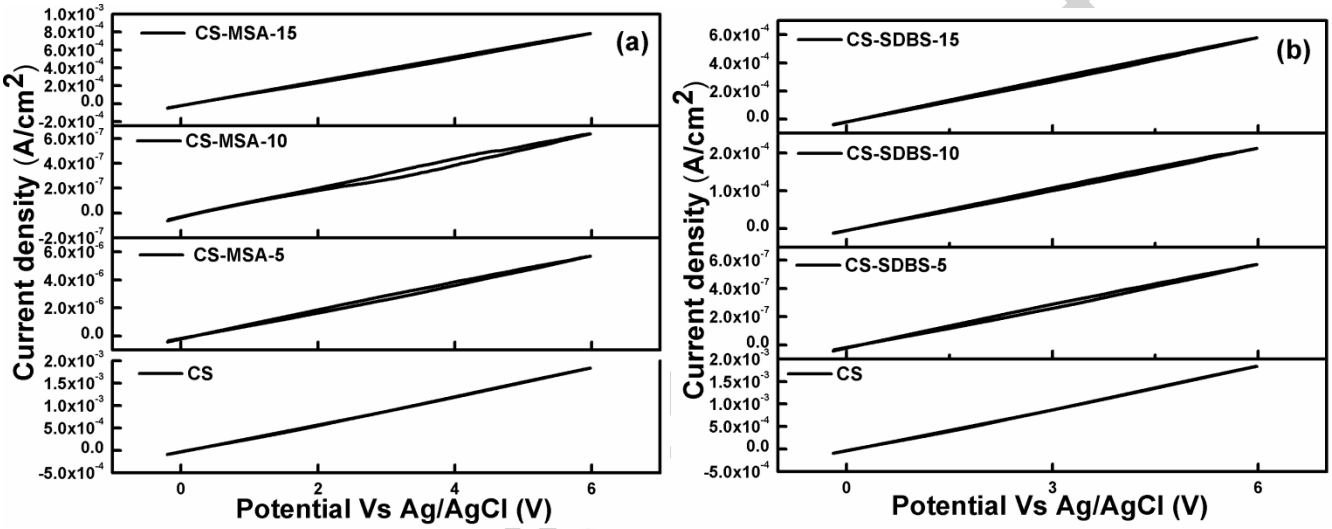

Fig. 12 I-V hysteresis curves of (a) CS-MSA and (b) CS-SDBS membranes

4.0 Summary and Conclusion

In summary, we developed sulfonic acid (MSA and SDBS) doped cross-linked chitosan membranes by solution casting method for PEMFC applications. The interaction among chitosan, dopants and cross linking agent are confirmed by FTIR and UV – visible spectroscopy. The doped sulfonic groups in chitosan improve the surface roughness of the membranes. All the doped membranes exhibit good flexibility and mechanical strength requirement both in dry and hydrated states. The water uptake and IEC of CS-MSA and CS-SDBS membranes increase as the loading of sulfonic acid dopant increases. Moreover, all the developed membranes revealing enough oxidative stability and thermal stability up to 260°C. The CS-SDBS-10 and CS-MSA-15 membranes show the best conductivity at high temperature (100°C) under the hydrated state. The incorporation of dopant within chitosan matrix significantly

improves the electrical resistance of developed membranes up to 10 wt% and 5wt% loading of MSA and SDBS respectively.

CS-MSA and CS-SDBS membranes exhibit better mechanical, thermal and hydrolytic stability which is comparable to standard Nafion membranes. However these membranes exhibit lower conductivity compared to Nafion membranes. But these membranes are derived from natural and biodegradable polymer, and these eco – friendly materials are more cost effective compared to Nafion.

References

[1] J.W. Lee, S.B. Khan, K. Akhtar, K.I. Kim, T.W. Yoo, Kwang-Won Seo, H. Han, A.M. Asiri, Fabrication of composite membrane based on silicotungstic heteropolyacid doped polybenzimidazole for high temperature PEMFC, Int. J. Electrochem. Sci. 7 (2012) 6276–6288.

[2] Q. Tang, J. Wu, Z. Tang, Y. Li, J. Lin, High-temperature proton exchange membranes from ionic liquid absorbed/doped superabsorbents, J. Mater. Chem. 22 (2012) 15836-15844.

[3] D.J. Kim, H.Y. Hwang, S. bong Jung, S.Y. Nam, Sulfonated poly(arylene ether sulfone)/Laponite-SO_3H composite membrane for direct methanol fuel cell, J. Ind. Eng. Chem. 18 (2012) 556–562

[4] S. Bose, T. Kuila, T.X.H. Nguyen, N.H. Kim, K. Lau, J.H. Lee, Polymer membranes for high temperature proton exchange membrane fuel cell: Recent advances and challenges, Prog. Polym. Sci. 36 (2011) 813–843.

[5] N.A. Aini, M.Z.A Yahya, A. Lepit, N.K. Jaafar, M.K. Harun, A. M.M. Ali, Preparation and characterization of UV irradiated SPEEK/chitosan membranes, Int. J. Electrochem. Sci. 7 (2012) 8226–8235.

[6] S. P. Nunes, Inorganic modification of proton conductive polymer membranes for direct methanol fuel cells, J. Memb. Sci. 203 (2002) 215–225.

[7] P. Kanakasabai, A.P. Deshpande, S. Varughese, Novel polymer electrolyte membranes based on semi-interpenetrating blends of poly(vinyl alcohol) and sulfonated poly(ether ether ketone)., J. Appl. Polym. Sci. 127 (2013) 2140–2151.

[8] Y. Wan, K. a M. Creber, B. Peppley, V.T. Bui, Chitosan-based electrolyte composite membranes. II. Mechanical properties and ionic conductivity, J. Memb. Sci. 284 (2006) 331–338.

[9] S.G.G. H. Yea, J. Huanga, J.J. Xua, N.K.A.C. Kodiweerab, J.R.P. Jayakodyb, 1, A, New membranes based on ionic liquids for PEM fuel cells at elevated temperatures, J. Power Sources. 178 (2008) 651–660.

[10] R. Devanathan, Recent developments in proton exchange membranes for fuel cells, Energy Environ. Sci. 1 (2008) 101-119.

[11] H. Liu, C. Gong, J. Wang, X. Liu, H. Liu, F. Cheng, G. Wang, G. Zheng, C. Qin, S. Wen, Chitosan/silica coated carbon nanotubes composite proton exchange membranes for fuel cell applications, Carbohydr. Polym. 136 (2015) 1379–1385.

[12] Y. Xiao, Y. Xiang, R. Xiu, S. Lu, Development of cesium phosphotungstate salt and chitosan composite membrane for direct methanol fuel cells, Carbohydr. Polym. 98 (2013) 233–240.

[13] Y. Wan, K. A. M. Creber, B. Peppley, V.T. Bui, Ionic conductivity of chitosan membranes, Polymer (Guildf). 44 (2003) 1057–1065

[14] P.B. Palani, K.S. Abidin, R. Kannan, M. Sivakumar, F.-M. Wang, S. Rajashabala, G. Velraj, Improvement of proton conductivity in nanocomposite polyvinyl alcohol (PVA)/chitosan (CS) blend membranes, RSC Adv. 4 (2014) 61781–61789.

[15] A. S. A Khiar, R. Puteh, a. K. Arof, Conductivity studies of a chitosan-based polymer electrolyte, Phys. B Condens. Matter. 373 (2006) 23–27.

[16] P.P. Sharma, V. Kulshrestha, Synthesis of highly stable and high water retentive functionalized biopolymer-graphene oxide modified cation exchange membranes, RSC Adv. 5 (2015) 56498–56506.

[17] I. A. Fadzallah, S.R. Majid, M. A. Careem, A. K. Arof, Relaxation process in chitosan–oxalic acid solid polymer electrolytes, Ionics (Kiel). 20 (2014) 969–975.

[18] F. Chen, P., Lai, Y., Kuo, T., Liu, J. Med. Biol. Eng. 27 (2007) 23–28.

[19] N.K. Idris, N. A N. Aziz, M.S.M. Zambri, N. A. Zakaria, M.I.N. Isa, Ionic conductivity studies of chitosan- based polymer electrolytes doped with adipic acid, Ionics (Kiel). 15 (2009) 643–646.

[20] B. Smitha, S. Sridhar, A.A. Khan, Synthesis and characterization of poly(vinyl alcohol)-based membranes for direct methanol fuel cell, J. Appl. Polym. Sci. 95 (2005) 1154–1163.

[21] S. Sumathi, V. Sethuprakhash, W.J. Basirun, A Comparative Studies on Methanesulfonic and p-Touluene Sulfonic Acid Incorporated Polyacrylamide Gel Polymer Electrolyte for Tin-Air Battery, Int J. Chemical, molecular, Nuclear, Materials and Metallurgical Eng. 7 (2013) 603-608.

[22] N. Rebert, B.G. Ateya, T. Poweigha, L.G. Austin, Some Electrochemical Properties of Strong Organic Acids for Use as Fuel Cell Electrolytes : Methane sulfonic, Methane di-silfonic, Trichloroacetic, Chloro-difluoroacetic, Pentafluoropropanoic, Benzoic and Benzene Sulfonic Acids, J.Electrochem. Soc. 127 (1980) 2641-2646

[23] P. Linganathan, J.M. Samuel, Effect of Dodecyl Benzene Sulphonic Acid on the Electrical Conductivity Behaviour of Poly (2-chloroaniline) and Poly (2-chloroaniline)/Silk Blends, 4 (2014) 107–116.

[24] M.D. Gernon, M. Wu, T. Buszta, P. Janney, Environmental benefits of methanesulfonic acid, Green Chem. 1 (1999) 127–140.

[25] A. Aysiha, R. Radhakrishnan, K. Prem Nazeer, Study of Structure-Property Relationship on Sulfuric Acid Crosslinked Chitosan Membranes, Malaysian Polym. J. 6 (2011) 27–38.

[26] P.O. Osifo, A. Masala, The Influence of Chitosan Membrane Properties for Direct Methanol Fuel Cell Applications, J. Fuel Cell Sci. Technol. 9 (2012) 1-9.

[27] C. Guo, L. Zhou, J. Lv, Effects of expandable graphite and modified ammonium polyphosphate on the flame-retardant and mechanical properties of wood flour-polypropylene composites, Polym. Polym. Compos. 21 (2013) 449–456.

[28] C.-H. Shen, S.L.-C. Hsu, E. Bulycheva, N. Belomoina, High temperature proton exchange membranes based on poly(arylene ether)s with benzimidazole side groups for fuel cells, J. Mater. Chem. 22 (2012) 19269-19275.

[29] K. Karuppasamy, R. Antony, S. Thanikaikarasan, S. Balakumar, X.S. Shajan, Combined effect of nanochitosan and succinonitrile on structural, mechanical, thermal, and electrochemical properties of plasticized nanocomposite polymer electrolytes (PNCPE) for lithium batteries, Ionics. 19 (2013) 747–755.

[30] F. Song, Y. Fu, Y. Gao, J. Li, J. Qiao, X. Zhou, Y. Liu, Novel Alkaline Anion-exchange Membranes Based on Chitosan / Ethenylmethylimidazoliumchloride Polymer with Ethenylpyrrolidone

Composites for Low Temperature Polymer Electrolyte Fuel Cells, Electrochimica Acta. 177 (2015) 137–139.

[31] J. Ostrowska-Czubenko, M. Pierog, M. Gierszewska-Druzynska, Water state in chemically and physically crosslinked chitosan membranes, J. Appl. Polym. Sci. 130 (2013) 1707–1715.

[32] B.P. Tripathi, T. Chakrabarty, V.K. Shahi, Highly charged and stable cross-linked 4,4’-bis(4-aminophenoxy)biphenyl-3,3'-disulfonic acid (BAPBDS)-sulfonated poly(ether sulfone) polymer electrolyte membranes impervious to methanol., J. Mater. Chem. 20 (2010) 8036–8044.

[33] Y. Xiang, M. Yang, Z. Guo, Z. Cui, Alternatively chitosan sulfate blending membrane as methanol blocking polymer electrolyte membrane for direct methanol fuel cell, J. Memb. Sci. 337 (2009) 318–323.

[34] M. A Witt, G.M.O. Barra, J.R. Bertolino, A. T.N. Pires, Crosslinked chitosan/poly (vinyl alcohol) blends with proton conductivity characteristic, J. Braz. Chem. Soc. 21 (2010) 1692–1698.

[35] M.C. Lin, H.Y. Tai, T.C. Ou, T.M. Don, Preparation and characterization of UV-sensitive chitosan for UV-cure with poly(ethylene glycol) dimethacrylate, Cellulose. 19 (2012) 1689–1700

[36] S. Winardi, S. Chandrabose, M. Ohnmar, Q. Yan, N. Wai, T. Mariana, M. Skyllas-kazacos, Sulfonated poly (ether ether ketone)-based proton exchange membranes for vanadium redox battery applications, J. Memb. Sci. 450 (2014) 313–322.

[37] M.S.M. Eldin, A. I. Hashem, A M. Omer, T.M. Tamer, Preparation , characterization and antimicrobial evaluation of novel cinnamyl chitosan Schiff base, Inter. J. Adv. research 3 (2015) 741–755.

[38] R.P. Pandey, V.K. Shahi, A N-o-sulphonic acid benzyl chitosan (NSBC) and N,N-dimethylene phosphonic acid propylsilane graphene oxide (NMPSGO) based multi-functional polymer electrolyte membrane with enhanced water retention and conductivity, RSC Adv. 4 (2014) 57200–57209.

[39] W.-F. Chen, Y.-C. Shen, H.-M. Hsu, P.-L. Kuo, Continuous channels created by self-assembly of ionic cross-linked polysiloxane–Nafion nanocomposites, Polym. Chem. 3 (2012) 1991-1995.

[40] H. Liu, C. Gong, J. Wang, X. Liu, H. Liu, F. Cheng, G. Wang, G. Zheng, C. Qin, S. Wen, Chitosan/silica coated carbon nanotubes composite proton exchange membranes for fuel cell applications, Carbohydr. Polym. 136 (2015) 1379–1385.

[41] M.M. Hasani-Sadrabadi, E. Dashtimoghadam, F.S. Majedi, S. Wu, A. Bertsch, H. Moaddel, P.

Renaud, Nafion/chitosan-wrapped CNT nanocomposite membrane for high-performance direct methanol fuel cells, RSC Adv. 3 (2013) 7337–7346.

[42] S. Lu, R. Xiu, X. Xu, D. Liang, H. Wang, Y. Xiang, Polytetra fluoroethylene (PTFE) reinforced poly (ethersulphone) – poly (vinyl pyrrolidone) composite membrane for high temperature proton exchange membrane fuel cells, 464 (2014) 1–7.

[43] P. Mukoma, B.R. Jooste, H.C.M. Vosloo, Synthesis and characterization of cross-linked chitosan membranes for application as alternative proton exchange membrane materials in fuel cells, J. Power Sources. 136 (2004) 16–23.

[44] T. Chakrabarty, A.K. Singh, V.K. Shahi, Zwitterionic silica copolymer based crosslinked organic–inorganic hybrid polymer electrolyte membranes for fuel cell applications, RSC Adv. 2 (2012) 1949.

[45] B. Liu, G.P. Robertson, D. Kim, M.D. Guiver, W. Hu, Z. Jiang, Aromatic Poly (ether ketone)s with Pendant Sulfonic Acid Phenyl Groups Prepared by a Mild Sulfonation Method for Proton Exchange Membranes Aromatic Poly (ether ketone) s with Pendant Sulfonic Acid Phenyl Groups Prepared by a Mild Sulfonation Method (2007) 1934–1944.

[46] S.J. Paddison, The modeling of molecular structure and ion transport in sulfonic acid based ionomer membranes, J. New Mater. Electrochem. Syst. 4 (2001) 197–207.

[47] S. Ghosh, S. Maity, T. Jana, Polybenzimidazole/silica nanocomposites: Organic-inorganic hybrid membranes for PEM fuel cell, J. Mater. Chem. 21 (2011) 14897-14906.

[48] C. Zhang, C.J. Li, G. Zhang, X.J. Ning, C.X. Li, H. Liao, C. Coddet, Ionic conductivity and its temperature dependence of atmospheric plasma-sprayed yttria stabilized zirconia electrolyte, Mater. Sci. Eng. B Solid-State Mater. Adv. Technol. 137 (2007) 24–30.

[49] A.N. Mondal, B.P. Tripathi, V.K. Shahi, Highly stable aprotic ionic-liquid doped anhydrous proton-conducting polymer electrolyte membrane for high-temperature applications, Journal of Materials Chemistry. 21 (2011) 4117 – 4124.

[50] M. Luqman, J.W. Lee, K.K. Moon, Y.T. Yoo, Sulfonated polystyrene-based ionic polymer-metal composite (IPMC) actuator, J. Ind. Eng. Chem. 17 (2011) 49–55.

Highlights

- Cost – effective and eco-friendly membranes
- First ever reported MSA - Sulphuric acid and SDBS – Sulfuric acid combination in Chitosan based PEMs
- Better flexibility, oxidative and thermal stability, improved proton exchange capacity and conductivity up to 100℃
- Decreased methanol uptake at higher methanol concentration ensures better methanol barrier property
- CS-SDBS-10 followed by CS-MSA-15 shows highest proton conductivity at higher temperature in hydrated conditions

Graphical abstract